A Markov Modelling Approach for Surgical Process Analysis in Cataract Surgery

Maartje E. Zonderland, Siebe Brinkhof, Irene C. Notting, Richard J. Boucherie, Fredrik Boer, and Gré P. M. Luyten

Abstract Variability of surgical times heavily affects efficiency and utilisation of the operating room. This chapter develops a data-driven mathematical model that characterises the actions of the surgical process and their contribution to the total surgical time, including variability. The model gives insight into the surgical process, without the need to analyse a large number of surgeries for application of statistical methods. A surgical flow chart of cataract surgery is constructed by observing 85 cataract surgeries performed at Leiden University Medical Center (LUMC), combined with expert opinion. Markov chain analysis, based on this flow chart, is used to analyse the surgical process. The model identifies the sources of delay and variability in the surgical process and provides a structured way of analysing surgeries. The obtained surgical time distribution approximates the empirical surgical time distribution of cataract surgeries performed in 2009 and 2010 at LUMC. The model developed in this chapter may be used to study the influence of modifications in the surgical process and to predict the resulting surgical times. It can easily be adapted to analyse future surgical processes or to represent different surgical procedures.

M. E. Zonderland (✉) · S. Brinkhof · R. J. Boucherie
Center for Healthcare Operations Improvement and Research, University of Twente, Enschede, The Netherlands
e-mail: M.E.Zonderland@utwente.nl

I. C. Notting · G. P. M. Luyten
Department of Ophthalmology, Leiden University Medical Center, Leiden, The Netherlands

F. Boer
Department of Anesthesiology, Leiden University Medical Center, Leiden, The Netherlands

1 Introduction

Operating room (OR) scheduling is an important challenge for most hospitals and has received considerable attention in the healthcare logistics literature. OR scheduling based on mean values of surgery durations omitting variability results in high expected OR overtime and surgeon idle time [2]. Deterministic and stochastic mathematical programming models, queueing models, simulation models and heuristic approaches have been widely used to study and improve OR scheduling [1, 5]. An important aspect of OR scheduling is an adequate prediction of the surgical times, based on patient and surgeon characteristics that involve uncertainty [16]. Prediction of the total surgical time may be obtained from historical data recorded in the hospital information system [4].

A surgical process is defined as a succession of surgical actions performed between the first incision and closure of the wound(s). The surgical path is a realisation of this process, with total surgical time being the sum of the duration of the surgical actions. The surgeon decides which surgical actions are performed; the so-called decision points may have major influence on the surgical time [16]. Prior to surgery, it is uncertain which actions will be performed, in which order and how much time each action will consume. A surgical plan based on, among others, the patient's physical status gives an indication of the surgical time. However, this estimation is subject to variation due to complications and other, usually uncontrollable, factors. These uncertainties may lead to multiple possible surgical paths, with different durations and likelihoods of occurrence [9, 19]. Adequate prediction of these surgical times is of utmost importance for OR scheduling.

This chapter develops a data-driven Markov modelling approach to characterise the distribution of the surgical times based on observations of the surgical actions in the surgical process. In addition, our Markov modelling approach may be used to predict the distribution of surgical times for future, novel surgical processes. The model decomposes the surgical process into well-defined surgical actions and possible subsequent actions, where its parameters may be obtained from observation, expert opinion or a combination thereof. The model is validated using observed cataract surgeries performed at Leiden University Medical Center (LUMC). Cataract surgery is selected to validate the Markov modelling approach, since its surgical time is relatively short, its surgical process involves a well-defined set of surgical actions, and cataract surgeries are carried out in sufficient numbers to obtain a large set of observations, which can readily be obtained from the operating microscope. Numerical results indicate a good fit of the surgical times predicted by our Markov model with realised surgical times.

This chapter is organised as follows. Section 2 provides a brief literature overview of surgical time variability and Markov models for surgical times. Section 3 provides a description of the cataract surgical process and our data collection approach resulting in the surgical flow chart that is the basis of our Markov modelling approach in Sect. 4. A detailed description of the surgical time distribution is included in Sect. 5, followed by our conclusions in Sect. 6.

2 Literature

The degree as well as the source of variability in surgical processes is a widely studied topic in literature since its first description in [14]. Since then, several statistical models have been proposed for modelling surgical procedure times, based on log-normal and normal distributions of the total surgical time or surgical actions [15]. Surgeons working at constant but different rates due to, for example, experience and the surgeon's natural speed introduce another source of variability as shown in [16] via the analysis of 46,322 surgical processes. Variability may also be the result of surgical process disruptions, i.e. deviations from the natural progression of a surgical path [18]. Surgical process disruptions affect the mental readiness of the surgeon, which is regarded as an important factor affecting patient outcomes, probably even more than technical skills or physical readiness. The number of these (usually) uncontrollable factors depends on the type of procedure [9]. The effects of disruptions on surgical time are categorised into one of six groups in [19]: instrument change, surgeon position change, nurse duty shift, conversation, phone/pager answering and extraneous interruption. The frequency and duration of each type of disruptive event were recorded and analysed; focus is on disruptions of the surgical process and their effect on variability in surgical time, but the surgical process itself is not studied in detail.

A few modelling approaches to analyse surgical processes were developed in literature. Hidden Markov models are developed in [6, 11, 12] to evaluate surgical skills in minimal invasive surgery. This is done by comparing the Markov model of experienced surgeons to that of residents at various levels of training [10]. The state space of the Markov model represents the possible different combinations of instruments used by each hand of the surgeon. The surgical actions are not specified; focus is on the combination of instruments used by residents, compared to staff surgeons. The resulting skill level is based on four equally weighted criteria: overall performance, economy of movement, tissue handling and the number of errors such as dropped needles. An approach based on sensor data for instrument use to predict the (remaining) surgical time is developed in [3], where the prediction uses data mining and process mining techniques to obtain the surgical flow chart.

This chapter develops a data-driven Markov model that enables a statistical evaluation of surgical processes, based on the flow chart of surgeries taking into account all possible surgical actions and paths. This model can be used to estimate surgical times of existing surgical processes, as well as surgical times for novel surgeries.

3 Cataract Surgery and Data Collection Approach

Age-related cataract is a very common cause of visual impairment in older adults. As the lens ages, it increases in weight and thickness. The centre of the lens (nucleus) undergoes compression and hardening, and the lens takes on a yellow

or brownish hue with advancing age. This is a cataract, and over time, it may grow larger, resulting in poor vision. The lens may be replaced to restore vision.

The exact surgical paths for cataract surgeries is of utmost importance for a complete description of the process. Therefore, for the cataract surgeries incorporated in the present paper, we provide a detailed description of these paths (see Fig. 1 for the flow chart). To remove the lens, a standard extracapsular cataract extraction is performed through a 3.0 mm beveled corneal or limbal incision with a disposable phaco knife. The anterior chamber is then filled with an Ophthalmic Viscosurgical Device (Healon OVD, Abbott Medical Optics, inc.), which can be done in multiple steps, and capsulorhexis is performed. The capsule of the lens is a layer of approximately 14 micrometres thick, which is very fragile. It is important that the remainder of the capsular bag is undamaged. If it tears, the lens will fall into the inner part of the eye. This is a major complication that delays the surgical process considerably. For the removal of the cataracteous lens, the Millennium Phacoemulsification equipment (Bausch&Lomb) is used. This technique uses an ultrasonically driven tip (phaco tip) to fragment the centre of the cataract. The lens fragments are removed by irrigation and aspiration. Here, it is even more important to leave the lens capsule undamaged since it is very sensitive in this stadium of the process, being unsupported due to the removed nucleus. Depending on the surgeon's preferences and patient characteristics, such as lens hardness, a divide-and-conquer or stop-and-chop technique can be used. During phacoemulsification relatively high amounts of energy are delivered which can potentially damage the eye. It is therefore important to use as little phaco energy as possible. Nevertheless, smaller particles – in general resulting from more sculpting – are easier to remove, decreasing the risk of damaging the capsular bag. Finally, cortex remnants are removed with a bimanual irrigation and aspiration instrument. The OVD is used to implant the new intraocular lens and is removed thereafter with irrigation and aspiration of the canula. Suturing of the corneal wound is not necessary as a rule.

A prospective case-series study was performed at the Department of Ophthalmology of the Leiden University Medical Center, Leiden, the Netherlands (LUMC). The study was performed in accordance with the principles of the Declaration of Helsinki. The medical ethical committee of LUMC (full name: Commissie Medische Ethiek Leids Universitair Medisch Centrum) approved this study (CME decision #CME09/028) and waived the requirement for written informed consent.

All surgeries were performed by four experienced surgeons and three residents from the LUMC and were performed in 2009 and 2010. A total of 44 male and 41 female patients were included, with average age 71. Due to the last resort function of the LUMC, a high level of co-morbidity was present. Therefore, these patients might not represent the average cataract surgery population. Two cameras were set up in the OR, the first in the microscope of the surgeon and the second in a corner of the OR, giving a good overview of the surgical team and their interactions. Prior to surgery, patients were informed about the recordings, which were anonymised afterwards. Informed consent was given, and recordings started when the eye was draped and the eyelid speculum was placed. Solely the patient's eye is visible on the video registration.
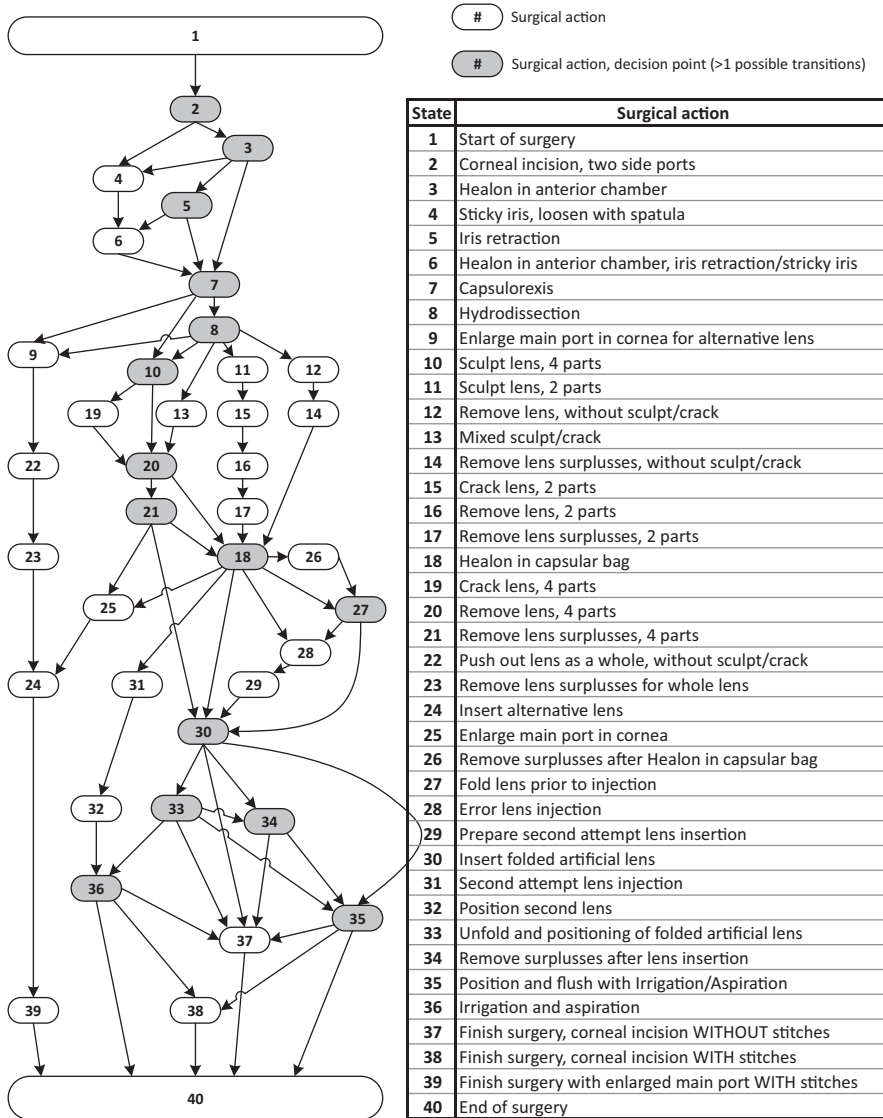
State	Surgical action
1	Start of surgery
2	Corneal incision, two side ports
3	Healon in anterior chamber
4	Sticky iris, loosen with spatula
5	Iris retraction
6	Healon in anterior chamber, iris retraction/stricky iris
7	Capsulorexis
8	Hydrodissection
9	Enlarge main port in cornea for alternative lens
10	Sculpt lens, 4 parts
11	Sculpt lens, 2 parts
12	Remove lens, without sculpt/crack
13	Mixed sculpt/crack
14	Remove lens surplusses, without sculpt/crack
15	Crack lens, 2 parts
16	Remove lens, 2 parts
17	Remove lens surplusses, 2 parts
18	Healon in capsular bag
19	Crack lens, 4 parts
20	Remove lens, 4 parts
21	Remove lens surplusses, 4 parts
22	Push out lens as a whole, without sculpt/crack
23	Remove lens surplusses for whole lens
24	Insert alternative lens
25	Enlarge main port in cornea
26	Remove surplusses after Healon in capsular bag
27	Fold lens prior to injection
28	Error lens injection
29	Prepare second attempt lens insertion
30	Insert folded artificial lens
31	Second attempt lens injection
32	Position second lens
33	Unfold and positioning of folded artificial lens
34	Remove surplusses after lens insertion
35	Position and flush with Irrigation/Aspiration
36	Irrigation and aspiration
37	Finish surgery, corneal incision WITHOUT stitches
38	Finish surgery, corneal incision WITH stitches
39	Finish surgery with enlarged main port WITH stitches
40	End of surgery

Fig. 1 Graphical representation of the cataract surgery flow chart, where arrows indicate possible transitions, and the table gives the corresponding surgical actions. The grey states indicate decision points, with more than one outgoing arrow

The process of cataract surgery in terms of surgical actions and their order of appearance is visualised by a surgical flow chart. Surgical actions are represented by circles and their order of appearance by arrows between actions. The time-action technique described in [7] is employed. Surgical actions that are performed by the

surgeon are registered in chronological order, with the start and end times of each action determined by analysis of the video registrations. After each surgery, the surgical process is discussed with the surgeon. The flow chart was constructed from video observations and expert opinion. Discussions with surgeons declared well-defined surgical actions with start and end point indications such as usage of a different instrument. Each observation defines a surgical path, and a combination of these paths may result in unobserved, but possible surgical paths. The resulting surgical flow chart of cataract surgery is given in Fig. 1. The legend specifies the corresponding surgical actions as defined from discussions with the staff surgeons.

4   Markov Model

Markov models are frequently used to analyse processes in which uncertainty plays an important role. For a comprehensive overview of Markov models, see [13, 17]. Our assumptions underlying the Markov modelling approach for surgical processes are the following:

(i) Each surgical process consists of a number of well-defined actions with start and end points.
(ii) Upon completion of a surgical action, the next action is selected from a well-defined set of possible actions, where selection of the next action is determined only by the current action.
(iii) The sojourn times of surgical actions are independent random variables with a normally distributed duration.

The surgical flow chart is used to develop a Markov model to analyse the surgical process. States represent surgical actions, and for each state the successive state is determined by transition probabilities. A possible sequence of states forms a surgical path. Each surgical action has a random duration with a corresponding probability distribution, for which we assume a normal distribution. The normal distribution is commonly used to characterise variables that tend to cluster around a mean with variability caused by small effects [13]. This assumption includes a positive probability of negative length. Nonetheless, the resulting errors may be negligible or within acceptable limits, allowing us to obtain a statistical estimation of surgical times with sufficient accuracy. Upon completion of a surgical action, there may be several possible subsequent actions from which the surgeon selects. Their fraction is modeled by transition probabilities. A more frequently selected action results in a higher value of the transition probability. Summarising, the Markov model has the following characteristics:

S State space of the Markov model containing all possible states of the process, representing the surgical actions of the surgical process.

$p_{i,j}$ Transition probabilities of the Markov process moving from state i to state j, representing the fraction of surgeries where surgical action j follows action i. This fraction may equal zero, which means that the two surgical actions cannot be in direct succession.

τ_i Random variable representing the time spent in state i (sojourn time) before the process progresses to the next state. The duration of a surgical action is described by this parameter. The normal probability distribution is used to model the variability in this parameter.

Assumption (ii) might seem unrealistic as decisions in decision points may differ due to previous surgical actions. If that is the case, then decision states will be separated into multiple states with their separate surgical actions and transition probabilities. As an illustration, consider state 18 in Fig. 1. If selection of the next states 25, 26, 27, 28 and 30 depends on the surgical path leading to state 18, then state 18 would be separated into states 18a, b and so on, with their own set of transition probabilities.

The surgical time equals the summation of the individual surgical action durations on a surgical path. For each (observed) surgical process, k the sequence of actions is registered in terms of the corresponding surgical flow chart. A sequence x_k defines the surgical path sequence. The associated durations of each action are also registered as a sequence: the surgical time sequence t_k. Let m_k define the number of actions in surgical process k, and denote:

$$\text{Surgical path sequence of surgical process } k : x_k = \{x_{k_1}, \ldots, x_{k_j}, \ldots, x_{k_{m_k}}\}, \quad (1)$$

$$\text{Surgical time sequence of surgical process } k : t_k = \{t_{k_1}, \ldots, t_{k_j}, \ldots, t_{k_{m_k}}\}, \quad (2)$$

i.e. x_{k_j} and t_{k_j} are the jth action and time in surgical process k. Due to the assumption of normally distributed sojourn times for each surgical action, the surgical time for each surgical path is a summation of normally distributed sojourn times and therefore also has a normal distribution [13]. If the sojourn time of surgical action i has a normal distribution with mean μ_i and variance σ_i^2, then the surgical time N_{x_k} of surgical path x_k has a normal distribution with mean μ_{x_k} and variance $\sigma_{x_k}^2$, given by

$$\mu_{x_k} = \sum_{i \in x_k} \mu_i, \quad (3)$$

$$\sigma_{x_k}^2 = \sum_{i \in x_k} \sigma_i^2. \quad (4)$$

The transition probabilities between surgical actions represent the fraction of times a surgeon selects a certain subsequent action. For example, if the transition probability from state i to state j equals 0.1, then surgeons select surgical action j following

action i in 10% of the surgeries. The probability of occurrence o_{x_k} of a particular surgical path x_k is obtained by multiplying the transition probabilities associated with the transitions in the surgical path. The probability of occurrence o_{x_k} of surgical path x_k with m_k surgical actions is given by

$$o_{x_k} = \prod_{j=1}^{m_{k-1}} p_{x_{k_j}, x_{k_{j+1}}}. \tag{5}$$

The total surgical time distribution T is a weighted combination of the surgical times of all possible surgical paths. Note that these paths include but are not restricted to the paths observed to determine the surgical flow chart. The weight of path x_k is its probability of occurrence o_{x_k}. Let X denote the set of all surgical paths (observed and unobserved). We thus obtain

$$T = \sum_{x \in X} o_x \cdot N_x. \tag{6}$$

5 Data Analysis and Results

From the observations of 85 cataract surgeries at the Department of Ophthalmology of the LUMC in 2009 and 2010, a total of 38 different surgical actions plus a start and end state are identified. Figure 1 gives all surgical actions and transitions between surgical actions that were observed. We identify 15 decision points indicated by the grey states, where multiple subsequent actions may be selected by the surgeon. To determine the characteristics of the Markov chain model for the surgical flow chart, from the observed data, we determine for each action i the mean μ_i and variance σ_i^2 using the standard estimator for the sample mean and sample variance for the normal distribution. Table 1 gives for each action the number of times the action was observed and the estimated mean and variance of the sojourn times. For some states the standard deviation is large with respect to the mean due to a relatively small number of observations. States 26, 31 and 32 are observed only once, so for these states the standard deviation cannot be estimated and is set to 0. The transition probabilities $p_{i,j}$ between action i and action j are determined for the decision points using the standard estimator for transition probabilities as the fraction of times action i was followed by action j. Table 2 gives the transition probabilities.

The number of possible paths in the flow chart of Fig. 1 is much larger than the observed number of 85 surgeries. Table 3 lists the number of possible paths from each decision state to the end of surgery in state 40. The total number of paths that may be identified from our observations is 7590, which clearly illustrates the complexity and the large number of possible surgical paths even for a surgical process with a small number of decision points such as cataract surgery.

Table 1 Mean, standard deviation of sojourn times and number of observations for the states in the cataract surgery model

State	Description	$\bar{x}$	SD	N
1	Start of surgery	0.0	0.0	85
2	Corneal incision, two side ports	38.0	29.0	85
3	Healon in anterior chamber	19.7	9.2	84
4	Sticky iris, loosen with spatula	78.0	23.3	3
5	Iris retraction	307.7	179.1	3
6	Healon in anterior chamber, iris retraction/sticky iris	42.0	44.0	5
7	Capsulorhexis	98.3	82.2	85
8	Hydrodissection	42.3	41.6	83
9	Enlarge main port in the cornea for alternative lens	265.5	71.5	2
10	Sculpt lens, 4 parts	168.0	103.3	59
11	Sculpt lens, 2 parts	59.0	17.7	13
12	Remove lens, without sculpt/crack	85.4	32.6	7
13	Mixed sculpt/crack	351.0	260.8	4
14	Remove lens surpluses, without sculpt/crack	205.7	66.8	7
15	Crack lens, 2 parts	29.3	14.3	13
16	Remove lens, 2 parts	151.2	73.4	13
17	Remove lens surpluses, 2 parts	176.7	75.8	13
18	Healon in capsular bag	24.0	12.5	81
19	Crack lens, 4 parts	56.2	56.9	57
20	Remove lens, 4 parts	141.3	97.1	63
21	Remove lens surpluses, 4 parts	251.3	144.8	62
22	Push out lens as a whole, without sculpt/crack	65.0	39.0	2
23	Remove lens surpluses for whole lens	665.0	102.0	2
24	Insert alternative lens	328.8	97.1	4
25	Enlarge main port in cornea	34.5	4.5	2
26	Remove surpluses after Healon in capsular bag	59.0	0.0	1
27	Fold lens prior to injection	87.6	16.0	7
28	Error lens injection	32.3	17.4	3
29	Prepare second attempt lens insertion	156.0	55.5	3
30	Insert folded artificial lens	34.3	30.6	80
31	Second attempt lens injection	142.0	0.0	1
32	Position second lens	19.0	0.0	1
33	Unfold and positioning of folded artificial lens	36.7	70.4	45
34	Remove surpluses after lens insertion	88.1	53.2	7
35	Position and flush with irrigation/aspiration	65.0	29.3	46
36	Irrigation and aspiration	63.9	32.1	28
37	Finish surgery, corneal incision WITHOUT stitches	72.8	60.8	60
38	Finish surgery, corneal incision WITH stitches	191.7	107.9	14
39	Finish surgery with enlarged main port WITH stitches	580.8	318.5	4
40	End of surgery	0.0	0.0	85

Table 2 Transition probabilities $p_{i,j}$ for the cataract surgery model

State	$p_{i,j}$	$p_{i,j}$	$p_{i,j}$	$p_{i,j}$	$p_{i,j}$	$p_{i,j}$
1	p(1,2)=1.0000					
2	p(2,3)=0.9882	p(2,4)=0.0118				
3	p(3,4)=0.0238	p(3,5)=0.0357	p(3,7)=0.9405			
4	p(4,6)=1.0000					
5	p(5,6)=0.6667	p(5,7)=0.3333				
6	p(6,7)=1.0000					
7	p(7,8)=0.9765	p(7,9)=0.0118	p(7,10)=0.0118			
8	p(8,9)=0.0120	p(8,10)=0.6988	p(8,11)=0.1566	p(8,12)=0.0843	p(8,13)=0.0482	
9	p(9,22)=1.0000					
10	p(10,19)=0.9661	p(10,20)=0.0339				
11	p(11,15)=1.0000					
12	p(12,14)=1.0000					
13	p(13,20)=1.0000					
14	p(14,18)=1.0000					
15	p(15,16)=1.0000					
16	p(16,17)=1.0000					
17	p(17,18)=1.0000					
18	p(18,25)=0.0123	p(18,26)=0.0123	p(18,27)=0.0741	p(18,28)=0.0247	p(18,30)=0.8642	p(18,31)=0.0123
19	p(19,20)=1.0000					
20	p(20,18)=0.0159	p(20,21)=0.9841				
21	p(21,18)=0.9677	p(21,25)=0.0161	p(21,30)=0.0161			
22	p(22,23)=1.0000					
23	p(23,24)=1.0000					
24	p(24,39)=1.0000					
25	p(25,24)=1.0000					
26	p(26,27)=1.0000					
27	p(27,28)=0.1429	p(27,30)=0.8571				
28	p(28,29)=1.0000					
29	p(29,30)=1.0000					
30	p(30,33)=0.5625	p(30,34)=0.0250	p(30,35)=0.4000	p(30,37)=0.0125		
31	p(31,32)=1.0000					
32	p(32,36)=1.0000					
33	p(33,34)=0.1111	p(33,35)=0.2667	p(33,36)=0.6000	p(33,37)=0.0222		
34	p(34,35)=0.2857	p(34,37)=0.7143				
35	p(35,37)=0.7609	p(35,38)=0.1522	p(35,40)= 0.0870			
36	p(36,37)=0.6429	p(36,38)=0.2500	p(36,40)=0.1071			
37	p(37,40)=1.0000					
38	p(38,40)=1.0000					
39	p(39,40)=1.0000					
40						

In 2009 and 2010 a total of 2041 cataract surgeries was carried out in the LUMC. A histogram of the realised surgical times as well as the best-fit surgical time distribution is depicted in Fig. 2a, c, where in Fig. 2c the solid line represents surgeries carried out by all surgeons and the dashed line surgeries carried out by staff surgeons only. Figure 2b shows a histogram of the realised surgical times of the 85 observed cataract surgeries.

To validate our Markov modelling approach, we compare our estimate of the surgical time distribution with that distribution for the realised surgeries in 2009

Table 3 Number of paths from decision states to end state 40

State	# of paths	State	# of paths	State	# of paths	State	# of paths	State	# of paths
1	7590	9	1	17	118	25	1	33	11
2	7590	10	512	18	118	26	38	34	4
3	6072	11	118	19	256	27	38	35	3
4	1518	12	118	20	256	28	19	36	3
5	3036	13	256	21	138	29	19	37	1
6	1518	14	118	22	1	30	19	38	1
7	1518	15	118	23	1	31	3	39	1
8	1005	16	118	24	1	32	3	40	

Table 4 Recorded length of cataract surgeries for different surgeons

Surgeon	Type	Observations (N)	Surgeries in 2009–2010 (N)	$\bar{x}$ surgical time (s)	SD surgical time (s)
1	Staff	12	251	805	496
2	Staff	14	541	1384	643
3	Staff	20	231	939	299
4	Staff	28	382	900	428
5	Residents	11	144	1536	432
Total		85	1549	1058	515

Not all surgeons that carry out cataract surgeries of LUMC were included, so the total number of surgeries (1549) is smaller than the 2041 surgeries that were used for the histogram of Fig. 2a

and 2010. As surgeons perform a varying number of surgeries per year, the fraction of the number of observations per surgeon in our sample set of logged data do not fully match the fractions of surgeries carried out by each surgeon in 2009 and 2010. Comparison of the surgical time distribution from our 85 observations with that from the 2041 realised surgeries should take into account the differences between surgical processes over surgeons and residents as the decisions made during surgery and the speed of actions may vary over surgeons. Therefore, to compare with the logged data from 2009 and 2010, the registered surgeries are weighted, such that the weight of the fraction of surgeries carried out by each surgeon in the 85 observed surgeries represents the weight of the total number of surgeries carried out by each surgeon in the observed period. Table 4 gives the number of surgeries carried out by four staff surgeons and residents, where we do not discriminate between residents. Observe the large differences both in mean and standard deviation of the surgical times. Not all surgeons who perform cataract surgeries of LUMC were included in Table 4, so the total number of surgeries (1549) is smaller than the 2041 surgeries that were used for the histogram of Fig. 2a. Figure 2d shows the surgical time distribution for the 2041 cataract surgeries carried out in LUMC in 2009 and 2010 (solid line) and the surgical time distribution from our Markov modelling approach taking into account the differences in handling speed and preferences between surgeons, as well as the influence of number of surgeries carried out by different surgeons (dashed line). These graphs show a striking match which illustrates the validity of our Markov modelling approach.
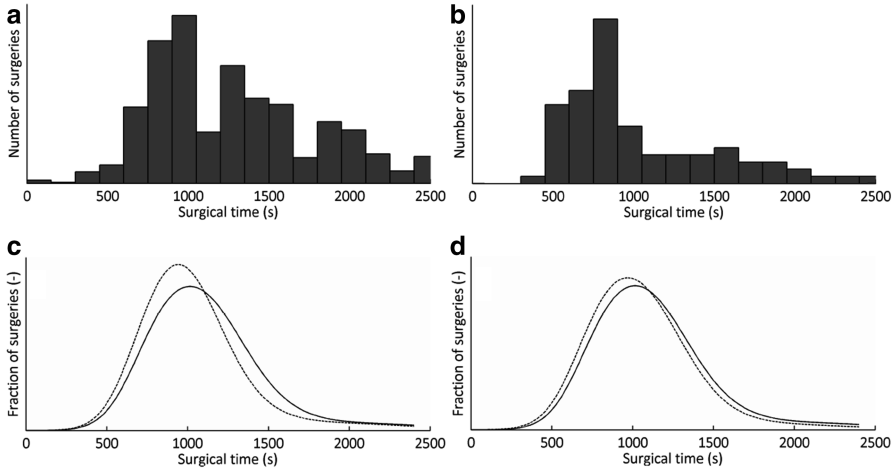
Fig. 2 Overview of realised and modeled surgical times. (**a**) Histogram of 2041 surgical time realisations in LUMC in 2009 and 2010. (**b**) Histogram of 85 surgical time realisations used to fit the model parameters. (**c**) Comparison of surgical time distributions of modeled surgical times for all surgeons (solid line) and staff surgeons only (dashed line). (**d**) Comparison of the observed surgical time distribution for the 2041 cataract surgeries in 2009 and 2010 (solid line) and the surgical time distributions from observations of 85 cataract surgeries taking into account the weighted fraction of surgeries carried out by different surgeons (dashed line)

The main characteristics of the surgical time distribution are captured by the Markov model. First, observe that each surgical path has a normally distributed surgical time. The surgical time distribution is a mixture of these surgical times. The mixture of random variables with a normal distribution is, in general, not normally distributed. Our model captures the skewness of the surgical time distribution (part (c) of Fig. 2). Second, the graphs of the predicted and observed surgical times (parts (a)–(c) of Fig. 2) do show a great level of similarity. The surgical time distribution obtained by the Markov model (part (c) of Fig. 2) and the histogram of realised surgical times (part (a) of Fig. 2), however, also show some discrepancy. There are two main explanations of this discrepancy. First, note that the number of observations used in this study is limited, so that estimates of times per surgical action and transition probabilities show considerable variance. Second, disruptions as categorised in [19] are only partly taken into account in the mathematical model. Most notably, interruptions of the surgical process are ignored; the recording was paused during interruptions. Such interruptions occur at random times with highly unpredictable duration. Incorporating these interruptions, which usually result in considerable delay, would likely have resulted in a more skewed surgical time distribution. Since the steps in the surgical process were used to obtain a model that allows for prediction of surgery times of (future) surgeries, it is legitimate to not take into account these interruptions.

6   Conclusions

The Markov model presented in this chapter reveals the structure of the surgical process for cataract treatment in terms of the possible sequences of surgical actions and their estimated durations. It provides a detailed description of the surgical process and predicts the total surgical time. The data- and knowledge-driven approach leads to a structured way of analysing surgeries in terms of process characteristics. The Markov model can be adapted to analyse future surgeries of different types. These models will give insight into the surgical process, without the need to analyse a large number of surgeries for application of statistical methods. Further analysis of the Markov model could enable the development of methods to decrease variability and skewness by standardising surgical paths, searching for optimal surgical paths and optimal solutions for complications during surgery. The Markov model appears to capture the total surgical time well. It requires detailed data about the surgical process, which is currently not often available. Healthcare data is exploding, and it is reasonable to assume that also data required for detailed Markov models for surgical processes will become available in the near future.

If prior to a surgery it is known which paths are likely to be chosen by the surgeon, the expected surgical time can be estimated by analysing these paths. Differences in preferences and speed between surgeons can be analysed as well and could serve as a model for benchmarking and learning. Residents are able to compare their surgical skills and working pace with those of staff surgeons. Part (c) of Fig. 2 shows such an application of the model. Here the surgical times for all surgeons and only staff surgeons are compared. A more detailed comparison for different groups or individual surgeons may be undertaken using the model. This was beyond the scope of the present study. Categorising patients pre-surgically, for example, on gender or age, can be used to estimate their surgical time based on the patient characteristics and might lead to improved OR scheduling. In addition, during surgery the remaining duration of the surgical process might be estimated from the analysis of the Markov chain from the current action to end of surgery. By doing so, this structured approach suits the need of modern healthcare facilities by increasing both operating room efficiency and patient comfort, through increased insight in the surgical process.

Measurement errors in the realised surgical time data were observed, due to unclear starting time indicators for the time registrations. Additional observations, to complete coverage of all possible surgical paths, would lead to a better validation of the model. Automation of the observation process would be interesting for further research, where recordings matched to the instruments that are used during the surgeries can be related to specific surgical actions. This can be used to automatically construct a state space and the definition of model parameters, as described in [8]. In particular, when analysing new surgical techniques, this approach may substantially reduce the efforts in obtaining logged data to construct a suitable Markov model.

References

1. Cardoen B, Demeulemeester E, Beliën J.: Operating room planning and scheduling: a literature review. Eur. J. Oper. Res. **201**, 921–932 (2010)
2. Denton, B., Gupta, D.: A sequential bounding approach for optimal appointment scheduling. IIE Transactions. **35**, 1003–1016 (2003)
3. Guédon, A.C.P., Paalvast, M., Meeuwsen, F.C., Tax, D.M.J., van Dijke, A.P., Wauben, L.S.G.L., van der Elst, M., Dankelman, J., van den Dobbelsteen, J.J.: It is Time to Prepare the Next patient? Real-Time Prediction of Procedure Duration in Laparoscopic Cholecystectomies. J. Med. Syst. **40**, 271 (2016)
4. Van Houdenhoven M., Hans E.W., Klein J., Wullink G., Kazemier G.: A Norm Utilisation For Scarce Hospital Resources: Evidence from Operating Rooms in a Dutch University Hospital.: J. Med. Syst. **31**, 231–236 (2007)
5. Hulshof, P.J.H., Kortbeek, N., Boucherie, R.J., Hans, E.W., Bakker, P.J.M.: Taxonomic classification of planning decisions in health care: a structured review of the state of the art in OR/MS. Health Syst. **1**,129–175 (2012)
6. Megali, G, Sinigaglia, S, Tonet, O, Dario, P.: Modelling and evaluation of surgical performance using hidden Markov models. IEEE Trans. Biomed. Eng. **53**, 1911–1919 (2006)
7. Minekus, J.P., Rozing, P.M., Valstar, E.R., Dankelman, J.: Evaluation of humeral head replacements using time-action analysis. J Shoulder Elbow Surg. **12**, 152–157 (2003)
8. Padoy, N, Blum, T, Ahmadi, S, Feussner, H, Berger, M, Navab,N.: Statistical modeling and recognition of surgical workflow. Med Image Anal. **16**, 632–641 (2012)
9. Parker, S.E., Laviana, A.A., Wadhera, R.K., Wiegmann, D.A., Sundt, T.M.: Development and evaluation of an observational tool for assessing surgical flow disruptions and their impact on surgical performance. World J. Surg. **34**, 353–361 (2010)
10. Rosen, J, Brown, J.D., Chang, L, Sinanan, M.N., Hannaford, B.: Generalized approach for modeling minimally invasive surgery as a stochastic process using a discrete Markov model. IEEE Trans. Biomed. Eng. **53**, 399–413 (2006)
11. Rosen, J, Hannaford, B, Richards, C.G., Sinanan, M.N.: Markov modeling of minimally invasive surgery based on tool/tissue interaction and force/torque signatures for evaluating surgical skills. IEEE Trans. Biomed. Eng. **48**, 579–591 (2001)
12. Rosen, J, Solazzo, M, Hannaford, B, Sinanan, M.: Task decomposition of laparoscopic surgery for objective evaluation of surgical residents' learning curve using hidden Markov model. Comp. Aided Surg. **7**, 49–61 (2002)
13. Ross, S.M.: A first course in probability. 4th ed. Macmillan College Pub. Co, New York (1994)
14. Rossiter, C.E., Reynolds, C.E.: Automatic monitoring of the time waited in out-patient departments. Med. Care **1**, 218–225 (1963)
15. Strum, D.P, May, J.H., Vargas, L.G.: Modeling the uncertainty of surgical procedure times: comparison of log-normal and normal models. Anesthesiology **92**,1160–1167 (2000).
16. Strum, D.P., Sampson, A.R., May, J.H., Vargas, L.: Surgeon and type of anesthesia predict variability in surgical procedure times. Anesthesiology **92**, 1454–1466 (2000)
17. Tijms, H.C.: A First Course in Stochastic Models. 1st ed. Wiley, Chichester (2003)
18. Wiegman, D.A., El Bardissi, A.W., Dearani, J.A., Daly, R.C., Sundt, T.M.: Disruptions in surgical flow and their relationship to surgical errors: an exploratory investigation. Surgery **142**, 658–665 (2007)
19. Zheng, B, Martinec, D.V., Cassera, M.A., Swanström, L.L.: A quantitative study of disruption in the operating room during laparoscopic antireflux surgery. Surg Endosc. **22**, 2171–2177 (2008)